

# Precision Measurement of the $\beta$ Asymmetry in Spin-Polarized $^{37}\text{K}$ Decay

B. Fenker,<sup>1,2</sup> A. Gorelov,<sup>3</sup> D. Melconian,<sup>1,2,\*</sup> J.A. Behr,<sup>3</sup> M. Anholm,<sup>3,4</sup> D. Ashery,<sup>5</sup> R.S. Behling,<sup>1,6</sup> I. Cohen,<sup>5</sup> I. Craiciu,<sup>3</sup> G. Gwinner,<sup>4</sup> J. McNeil,<sup>7,3</sup> M. Mehlman,<sup>1,2</sup> K. Olchanski,<sup>3</sup> P.D. Shidling,<sup>1</sup> S. Smale,<sup>3</sup> and C.L. Warner<sup>3</sup>

<sup>1</sup>*Cyclotron Institute, Texas A&M University, 3366 TAMU, College Station, Texas 77843-3366, USA*

<sup>2</sup>*Department of Physics and Astronomy, Texas A&M University,  
4242 TAMU, College Station, Texas 77843-4242, USA*

<sup>3</sup>*TRIUMF, 4004 Wesbrook Mall, Vancouver, British Columbia V6T 2A3, Canada*

<sup>4</sup>*Department of Physics and Astronomy, University of Manitoba, Winnipeg, Manitoba R3T 2N2, Canada*

<sup>5</sup>*School of Physics and Astronomy, Tel Aviv University, Tel Aviv 69978, Israel*

<sup>6</sup>*Department of Chemistry, Texas A&M University,  
3012 TAMU, College Station, Texas 77843-3012, USA*

<sup>7</sup>*Department of Physics and Astronomy, University of British Columbia, Vancouver, British Columbia V6T 1Z1, Canada*  
(Dated: February 24, 2022)

Using TRIUMF's neutral atom trap, TRINAT, for nuclear  $\beta$  decay, we have measured the  $\beta$  asymmetry with respect to the initial nuclear spin in  $^{37}\text{K}$  to be  $A_\beta = -0.5707(13)_{\text{syst}}(13)_{\text{stat}}(5)_{\text{pol}}$ , a 0.3% measurement. This is the best relative accuracy of any  $\beta$ -asymmetry measurement in a nucleus or the neutron, and is in agreement with the standard model prediction  $-0.5706(7)$ . We compare constraints on physics beyond the standard model with other  $\beta$ -decay measurements, and improve the value of  $V_{\text{ud}}$  measured in this mirror nucleus by a factor of 4.

PACS numbers: 23.40.Bw, 32.80.Pj, 12.15.-y, 12.60.-i, 13.30.Ce, 14.60.St  
Keywords:  $\beta$  decay, atom trap, optical pumping,  $\beta$  asymmetry

Nuclear  $\beta$ -decay correlation experiments were instrumental in establishing the standard model (SM) charged weak interaction as a theory with spin-1  $W^\pm$  bosons, coupling only to left-handed neutrinos through a vector minus axial-vector ( $V-A$ ) current. Precision measurements continue to probe this structure [1]. Extensions to the SM propose that parity symmetry, which is maximally violated in the weak interaction, is restored at some higher energy scale by extending the  $SU(2)_L \otimes U(1)_Y$  electroweak gauge group to include a right-handed  $SU(2)_R$  sector. Manifest left-right symmetric models have an angle  $\zeta$  which mixes the weak ( $W_{L,R}$ ) eigenstates to form mass eigenstates with masses  $M_{1,2}$ , characterized by  $\delta = (M_1/M_2)^2$  [2].

Atom and ion trapping techniques [3–6], and progress in neutron decay measurements [7, 8], have allowed correlation parameters in  $\beta$  decay to be measured with improved precision recently, increasing their sensitivity as probes of non-SM physics. We present here an experiment combining a magneto-optical trap (MOT) with optical pumping (OP) to produce a set of nearly ideal conditions: an isomerically selected source of highly polarized [9]  $\beta$ -decaying atoms that are cold and localized within an exceptionally open geometry. We measure the correlation between the spin of a parent  $^{37}\text{K}$  nucleus and the momentum of the outgoing  $\beta^+$ , given by the decay rate [10]:

$$\frac{d^3\Gamma_{\text{angular}}}{dE_\beta d\Omega_\beta} \propto 1 + b \frac{m_e}{E_\beta} + \mathbf{P}_{\text{nucl}} \cdot \left( A_\beta \frac{\mathbf{p}_\beta}{E_\beta} \right), \quad (1)$$

where we have neglected terms that cancel in the asymmetry measurement of our geometry. In this expression,  $m_e$ ,  $E_\beta$ , and  $\mathbf{p}_\beta$  are the mass, total energy, and momen-

tum of the positron,  $\mathbf{P}_{\text{nucl}}$  is the polarization of the parent nucleus, and  $b$  and  $A_\beta$  are correlation parameters whose values depend on the symmetries inherent in the weak interaction. We take the SM value  $b = 0$  for this Letter, consistent with the  $E_\beta$  dependence of our observed asymmetry as shown below. We will consider non-SM physics that depend on  $E_\beta$  in a future publication [11].

The  $\beta$  asymmetry has been measured previously in the neutron and ten different nuclei. The focus of this work is the mixed  $I^\pi = 3/2^+ \rightarrow 3/2^+$  Fermi/Gamow-Teller  $\beta^+$  decay of  $^{37}\text{K}$ , which has a half-life of 1.236 51(94) s [12] and  $Q_{\text{EC}} = 6.147 47(23)$  MeV [13]. The transition to the ground state of  $^{37}\text{Ar}$  dominates with a branching ratio of 97.99(14)% [14]. The next most significant branch is to an excited  $5/2^+$  state at 2.7961 MeV, which must be pure GT with a value of  $A_\beta^{\text{GT}} = -0.6$ . All other branches to excited states are below 0.03% [15].

The corrected comparative half-life for  $^{37}\text{K}$  is  $\mathcal{F}t = 4605.4 \pm 8.2$  s [12] based on the half-life, branching ratio and  $Q_{\text{EC}}$  values given above. The  $\mathcal{F}t$  values for transitions between  $T = 1/2$  isospin doublets in mirror nuclei are related to the  $\mathcal{F}t$  value for  $0^+ \rightarrow 0^+$  decays via:

$$\mathcal{F}t^{\text{mirror}} = \frac{2\mathcal{F}t^{0^+ \rightarrow 0^+}}{1 + \frac{f_A}{f_V} \rho^2}, \quad (2)$$

where  $f_A/f_V = 1.0046(9)$  [14] is the ratio of statistical rate functions for axial-vector and vector currents, and  $\rho = \frac{C_A M_{\text{GT}}}{C_V M_F}$  is the ratio of Gamow-Teller and Fermi coupling constants ( $C_A/C_V$ ) and matrix elements ( $M_{\text{GT}}/M_F$ ). Equation (2) with  $\mathcal{F}t^{0^+ \rightarrow 0^+} = 3072.27(72)$  s [16] leads to  $\rho = 0.5768(21)$ .

For mixed transitions, the  $\beta$  asymmetry including the

possibility of right-handed currents is given by [10, 17]:

$$A_\beta = \frac{\frac{\rho^2(1-y^2)}{1+y} - 2\rho\sqrt{\frac{1}{1+y}}(1-xy)}{(1+x^2) + \rho^2(1+y^2)}, \quad (3)$$

where  $x \approx (\delta - \zeta)/(1 - \zeta)$  and  $y \approx (\delta + \zeta)/(1 + \zeta)$  are nonzero in left-right symmetric models. The SM prediction for  $^{37}\text{K}$  is found by setting  $x=y=0$ . With the above value of  $\rho$  derived from the measured  $\mathcal{F}t$  value, the result is  $A_\beta^{\text{SM}} = -0.5706(7)$ . The value and sign of  $\rho$  is such that the sensitivity of  $A_\beta$  to its uncertainty is reduced compared to other observables; e.g., for the  $\nu$  asymmetry it is nearly  $2\times$  bigger,  $B_\nu^{\text{SM}} = -0.7701(18)$ . The value of  $\rho$  varies considerably among  $^{37}\text{K}$  and the other well-studied mirror nuclei ( $^{19}\text{Ne}$ ,  $^{21}\text{Na}$  and  $^{35}\text{Ar}$ ) making each nucleus complementary to the others as each will have different dependencies on beyond the SM physics.

Recoil-order and radiative corrections to  $A_\beta$  [18] are included in our analysis. For isobaric analog decays, the induced 1st-order tensor form factor is very small (only present because of isospin symmetry breaking), and all but the very small induced pseudoscalar and  $q^2$  expansion of the Fermi and Gamow-Teller form factors [19] are given by the conserved vector current (CVC) hypothesis using measured electromagnetic moments [18]. These corrections combine to add  $\approx -0.0028E_\beta/E_0$  to the expression for  $A_\beta$ .

The experiment described here was performed with the TRIUMF Neutral Atom Trap (TRINAT) [20, 21]. TRIUMF's radioactive ion beam facility, ISAC, delivered  $8 \times 10^7$   $^{37}\text{K}$  ions/s, 0.1% of which were neutralized and trapped. Background from the decay of untrapped atoms in the collection MOT was avoided by pushing the trapped atoms every second by a pulsed laser beam to a second MOT [22] where the precision measurement took place, depicted in Fig. 1.

Once the atoms are collected in the second MOT, we apply a sub-Doppler cooling scheme unique to potassium [23]. Since the atoms can only be polarized while the MOT is off, we alternate between periods of trapping and polarizing the atoms. To optimize the shutoff time of the MOT's magnetic field, we employ an alternating-current MOT (ac MOT) [24]. Once atoms are pushed from the first trap and cooled, a series of 100 cycles begins, where each cycle consists of 1.9ms of polarizing the  $^{37}\text{K}$  nuclei and collecting polarized decay data, followed by 3.0ms of re-collecting the atoms with the ac MOT. This cycle is repeated with the polarization direction ( $\sigma^\pm$ ) flipped every 16s.

While the MOT light and magnetic fields are off, we optically pump the atoms on the  $D_1$  ( $4s_{1/2} \rightarrow 4p_{1/2}$ ) transition with circularly polarized light. This technique directly polarizes the nucleus via the hyperfine coupling of the atomic and nuclear spins. It also lets us measure  $P_{\text{nuc}}$  nondestructively by probing the atoms with a pulsed 355nm UV laser and detecting the resulting photoions

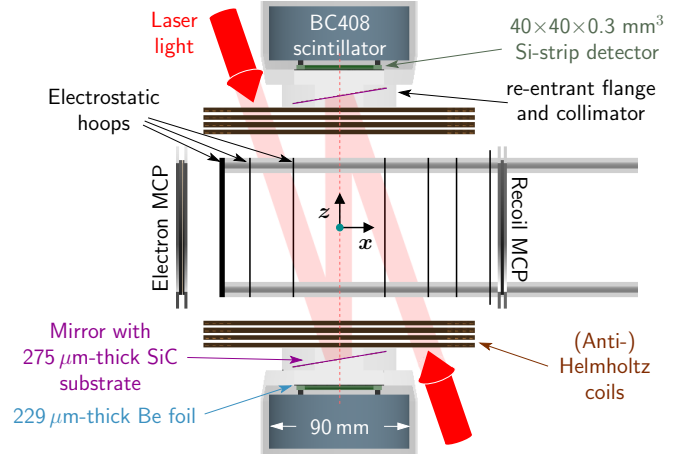


FIG. 1. The TRINAT detection chamber. To polarize the atoms along the  $\beta$ -detection ( $\hat{z}$ -) axis, optical pumping light is brought in at a  $19^\circ$  angle with respect to the  $\hat{z}$  axis and reflected off thin mirrors mounted within a  $\beta$  collimator on the front face of the reentrant flanges. Thin Be foils behind the mirrors separate the Si strip and scintillator  $\beta$  detectors from the  $1 \times 10^{-9}$  Torr vacuum of the chamber. Magnetic field coils provide the Helmholtz (optical pumping, 2 Gauss) and anti-Helmholtz (MOT) fields. Glassy carbon and titanium electrostatic hoops produce a uniform electric field of 150 to 535 V/cm in the  $\hat{x}$  direction to guide shakeoff electrons and ions towards microchannel plate detectors.

with the recoil MCP detector. The UV photons can only ionize atoms from the  $4p$  excited state which fully polarized atoms cannot populate, so the rate of photoions is a sensitive probe of  $P_{\text{nuc}}$ . Since  $1 - P_{\text{nuc}}$  is small, its determination to 10% precision is sufficient to achieve [9, 25]:  $P_{\text{nuc}}^{\sigma^+} = 99.13(8)\%$  and  $P_{\text{nuc}}^{\sigma^-} = -99.12(9)\%$ .

The time of flight (TOF) between the photoions and the UV laser pulse images the trap along  $\hat{x}$ , while a delay-line anode readout of the MCP provides position sensitivity to image the other axes. Since the MOT's cycling transition produces a relatively large fraction of atoms in the  $4p$  state, the position of the atoms is well known while the MOT is on. When the MOT light is off, very few atoms are available to be photoionized, and the trap position must be inferred from observations immediately before and after the polarized phase. From these measurements, we observed that the atom cloud moved  $0.37(5)\text{mm}$  while expanding from a volume of  $2.67(8)\text{mm}^3$  to  $16.9(3)\text{mm}^3$ . The entire cloud was illuminated by the OP light of 20 mm diameter ( $1/e^2$ ) throughout the optical-pumping cycle.

To identify decays that occurred within the region of optical pumping, we detect the low-energy shakeoff electrons (SOE) by sweeping them with an electric field towards an MCP and observing them in coincidence with the  $\beta^+$ . At least one SOE is present for every  $\beta^+$  decay [28, 29] because the  $\text{Ar}^-$  ion is unstable.

To detect the nuclear decay products, we employ a

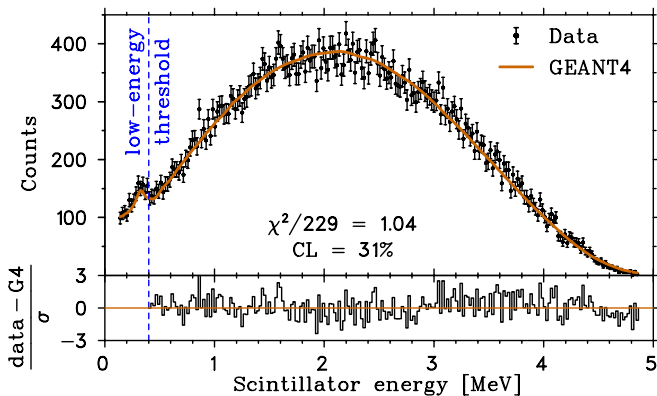


FIG. 2. Scintillator spectrum in coincidence with its DSSSD and the electron MCP, showing a very clean selection of  $\beta$ -decay events originating from the trapping region. The GEANT4 comparison shows residuals consistent with statistics. The vertical dashed blue line shows the energy threshold used to exclude Compton-scattered annihilation radiation.

pair of  $\beta$  telescopes along the vertical polarization axis (Fig. 1). Each consists of a thin double-sided Si-strip detector (DSSSD) backed by a 35-mm thick BC408 scintillator. The 300- $\mu$ m thick DSSSDs are segmented into 1-mm strips on both sides, providing position and  $\Delta E$  information. Because of its low efficiency for detecting  $\gamma$  rays, it also suppresses the background from 511-keV annihilation radiation.

The plastic scintillators and DSSSDs were calibrated by comparing the observed spectra to a GEANT4 simulation. For the plastic scintillators, we assumed a linear calibration and a detector resolution with a  $1/\sqrt{E}$  dependence. The calibration was performed using the scintillator spectrum in coincidence with a SOE without adding the energy deposited in the DSSSD. The calibration spectrum included both  $\beta^+$  events and the Compton edge of the 511-keV annihilation radiation. The resulting spectra including the DSSSD coincidence, shown in Fig. 2 for one detector, agree well with the simulation over the entire observed  $E_\beta$  range.

The asymmetry is calculated by comparing the observed rate of  $\beta$  particles in the two detectors. Since the experiment uses two symmetric detectors and reverses the sign of the polarization, we use the superratio technique which reduces many systematic uncertainties (see Refs. [30, 31] for details).

The data analysis was performed blind by temporarily culling an unknown fraction, up to 1%, of  $\beta$ -decay events from the analysis. All analysis cuts, corrections, and uncertainties were finalized on the biased data. The complete data set was then reanalyzed in this predefined way to obtain the final results presented here.

A detailed representation of the geometry of Fig. 1 was included in the GEANT4 simulation [32, 33]. The position of each decay was randomly sampled from the

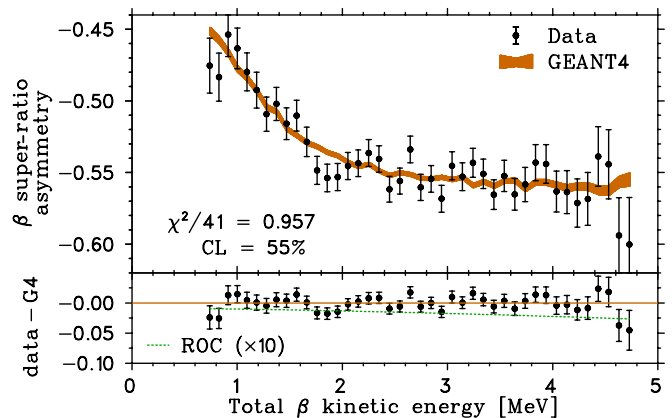


FIG. 3. Top: The physics superratio of a subset of the data (points) fit to a GEANT4 simulation (filled band, with the width indicating its statistical uncertainty) where the only free parameter was the value of  $\rho$ . Bottom: Difference between the data and GEANT4, and the small size of the recoil-order+radiative corrections (ROC).

observed distribution, modeled as a Gaussian ellipsoid and included the effects of the cloud's expansion and drift. We used the `emstandard_opt3` variation of the standard physics lists as well as nondefault values of 1  $\mu$ m for the cut-for-secondaries parameter and a range factor of  $f_R = 0.002$  in order to simulate the low- $E_\beta$  scattering of  $\beta^+$  more accurately [34]. The multiple scattering (MSC) of  $e^\pm$  was simulated with the Urban MSC model of Ref. [35] to avoid the nonphysical behavior of the Goudsmit-Saunderson MSC model [36] observed in Ref. [34].

The simulation was tested by directly comparing the fraction of  $\beta^+$  that backscattered out of the plastic scintillator. A large fraction of these events have the distinct signature of depositing energy in two different pixels of the DSSSD. The number of these backscattered events, normalized by the number of events leaving energy only in one pixel, was found to differ by only  $(2.6 \pm 1.3)\%$  from the measured values [25].

Events are considered in the asymmetry analysis if they (i) occur during the portion of the duty cycle that the atoms are fully polarized, (ii) have a valid DSSSD hit as well as energy deposited in the scintillator, and (iii) are in coincidence with a SOE. The four spectra for upper (lower) detector and spin up (down) are compared at a number of energy bins using the superratio technique to calculate the observed asymmetry shown in Fig. 3. The energy dependence is dominated by the  $\beta$ 's finite helicity [ $p_\beta/E_\beta$  of Eq. (1)]. The observed asymmetry is compared to the GEANT4 simulation in order to obtain the best-fit results for the input asymmetry.

Although our geometry is very open,  $\beta$  scattering off of volumes such as the opposite  $\beta$  telescope, electrostatic hoops, etc. (see Fig. 1), must be accounted for by GEANT4. Simulations indicate that 1.60% of accepted

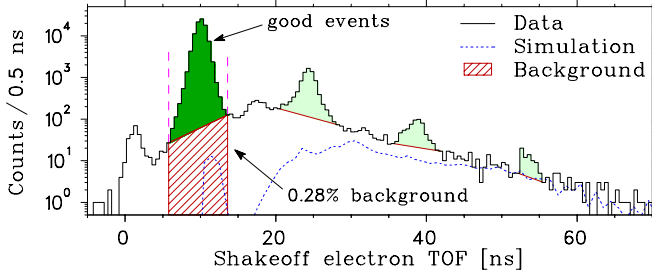


FIG. 4. Shakeoff electron TOF spectrum with respect to the  $\beta^+$ , showing all data at an electric field of 150 V/cm. This spectrum constrains the production of metastable  $\text{Ar}^-$  with  $\tau = 260(25)$  ns [37] to be less than 4%, while the TOF cut eliminates any possible contribution. Overlaid is a simulation (dotted line) of the TOF from atoms that escaped the trap before decaying from an electrostatic hoop, where the only free parameter is the normalization fixed to times  $\geq 43$  ns. While this simulation reproduces the longer TOF very well, it does not explain all of the background (red hatched area) under the main peak of good events within our TOF cuts (dashed vertical lines).

events scattered by  $\geq 24^\circ$  before being detected, leading to an effective  $\langle \cos \theta \rangle = 0.9775$  [25, 33]. The GEANT4 simulations therefore apply a 2.30% correction due to  $\beta$  scattering. Using a combination of our data and some from the literature, we assign a systematic uncertainty which is 5.6% of the correction (see Table I), as explained in the Supplemental Material [25].

Accounting for our measured  $\langle P \rangle = 99.13(9)\%$  [9], a simultaneous fit to all of our data yields a best-fit value  $A_{\text{obs}} = -0.5699(13)$  with  $\chi^2/123 = 0.82$ .

The TOF spectrum of SOEs with respect to the  $\beta^+$  (Fig. 4) has the expected large, narrow peak near  $t = 10$  ns, the good events we use in our analysis. The peaks at 24, 39, and 53 ns come from electrons that do not fire the MCP, but produce a secondary  $e^-$  that is re-collected by the electric field which is registered by the MCP. We can simulate most of the broad TOF structure to be background from decays of atoms stuck to the SiC mirrors and electrostatic hoops. The same simulation suggests an unresolved peak at 12 ns from the electrode nearest the trapping region, but this does not account for the majority of the total background under the good peak: 0.28%. We conservatively assume that this unknown background is either fully polarized or unpolarized atoms and make a correction  $A_\beta = A_{\text{obs}} \times 1.0014(14)$ .

Although the superratio technique greatly reduces the systematic uncertainties (e.g. the cloud position,  $\beta$  detector differences, and  $\beta$  scattering), this cancellation is not exact. Independently, we adjusted the trap position, size, temperature, drift velocity, and other parameters within the GEANT4 simulation, obtaining the systematic uncertainties shown in Table I.

TABLE I. Uncertainty budget for  $A_\beta$ . Each entry is given as the absolute uncertainty, and correction factors and the range varied are listed where applicable. Polarization uncertainties, detailed in Ref. [9], are statistically independent.

Source	Correction	Uncertainty
Systematics		
Background	1.0014	0.0008
$\beta$ scattering <sup>a</sup>	1.0230	0.0007
Trap ( $\sigma^+$ vs $\sigma^-$ )	$\left\{ \begin{array}{l} \text{position (typ } \lesssim \pm 20 \mu\text{m}) \\ \text{sail velocity (typ } \lesssim \pm 30 \mu\text{m/ms}) \\ \text{temperature (typ } \lesssim \pm 0.2 \text{ mK}) \end{array} \right.$	$\left. \begin{array}{l} 0.0004 \\ 0.0005 \\ 0.0001 \end{array} \right\}$
Si-strip	$\left\{ \begin{array}{l} \text{radius}^a (15.5^{+3.5}_{-5.5} \text{ mm}) \\ \text{energy agreement } (\pm 3\sigma \rightarrow \pm 5\sigma) \\ \text{threshold } (60 \rightarrow 40 \text{ keV}) \end{array} \right.$	$\left. \begin{array}{l} 0.0004 \\ 0.0002 \\ 0.0001 \end{array} \right\}$
Shakeoff electron TOF region ( $\pm 3.8 \rightarrow \pm 4.6$ ns)		0.0003
Thicknesses	$\left\{ \begin{array}{l} \text{SiC mirror}^a (\pm 6 \mu\text{m}) \\ \text{Be window}^a (\pm 23 \mu\text{m}) \\ \text{Si-strip}^a (\pm 5 \mu\text{m}) \end{array} \right.$	$\left. \begin{array}{l} 0.0001 \\ 0.00009 \\ 0.00001 \end{array} \right\}$
Scintillator only vs. $E + \Delta E^a$		0.0001
Scintillator threshold (400 $\rightarrow$ 1000 keV)		0.00003
Scintillator calibration ( $\pm 0.4$ ch/keV)		0.00001
Total systematics		0.0013
Statistics		0.0013
Polarization	1.0088	0.0005
Total	1.0338	0.0019

<sup>a</sup>Denotes sources that are related to  $\beta^+$  scattering.

The final result is

$$A_\beta = -0.5707(13)_{\text{syst}}(13)_{\text{stat}}(5)_{\text{pol}}, \quad (4)$$

where the third uncertainty combines the systematic and statistical uncertainties on the polarization measurement [9]. This result has the lowest relative uncertainty of any measurement of the  $\beta$  asymmetry in a nuclear system to date. Since the simulation includes the recoil-order and radiative corrections, this result may be directly compared to  $A_\beta^{\text{SM}}$  given earlier.

Figure 5 shows the allowed parameter space in the manifest left-right model. We vary  $\rho$  at each  $(\zeta, \delta)$  coordinate to minimize the  $\chi^2$  over all observables ( $\mathcal{F}t$ ,  $A_\beta$  and  $B_\nu$ ). The  $^{37}\text{K}$  limit includes our previous  $B_\nu$  measurement [38], but is dominated by the present  $A_\beta$  result.

Assuming  $\zeta = 0$  from other experiments (particularly Ref. [16]), our result implies  $\delta = 0.004^{+45}_{-4}$  and a mass for a  $W_R$  coupling to right-handed  $\nu^R$  greater than  $340 \text{ GeV}/c^2$  at 90% confidence, a slight improvement over the  $P_\beta/A_\beta$   $310 \text{ GeV}/c^2$  limit [2, 40]. Much of the parameter space in left-right symmetric models has been excluded by other measurements. Constraints from polarized muon decay [48] are relaxed if the  $\nu_\mu^R$  is heavy (as e.g. in Ref. [49]). LHC searches directly exclude  $W_R$  with mass  $< 3.7 \text{ TeV}/c^2$  if the right-handed gauge coupling  $g_R = g_L$  [39], while our  $^{37}\text{K}$  results imply  $g_R < 8$  for a  $4 \text{ TeV}/c^2$   $W_R$ . Manifest models with  $M_{W'} < M_W$  and



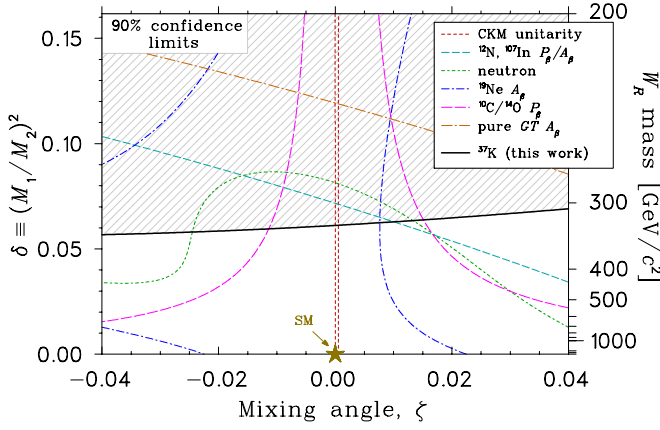


FIG. 5. Constraints on manifest L-R symmetric models from nuclear and neutron [39]  $\beta$  decay: CKM unitarity [16]; the ratio of  $\beta^+$  polarization to  $A_\beta$  of  $^{12}\text{N}$  and  $^{107}\text{In}$  [2, 40];  $A_\beta$  of mixed GT/F  $^{19}\text{Ne}$  [14, 41–43]; the  $\beta^+$  polarization of  $^{10}\text{C}$  compared to  $^{14}\text{O}$  [44]; and the weighted average of  $A_\beta$  from three recent pure-GT cases [45–47].

$V_{\text{ud}}^R$  considerably less than unity are also constrained by  $\beta$  decay correlations [2].

If we make the assumption that the SM completely describes the  $\beta$  decay of  $^{37}\text{K}$ , we can use the result to test the CVC hypothesis. Combining the present result for  $A_\beta$  with the previous measurement of  $B_\nu$  [38], we find  $\rho = 0.576(6)$ . This, in combination with the  $\mathcal{F}t$  value of Ref. [12], leads to  $V_{\text{ud}} = 0.9744(26)$  for  $^{37}\text{K}$ , a greater than  $4\times$  improvement over the previous value [12]. Isospin-mixing calculations [14] contribute 0.0004 to this uncertainty, which only grows to 0.0005 if the span between the isospin-tuned shell model of Ref. [14] and the density functional of Ref. [50] is taken as the uncertainty. We compare this determination of  $V_{\text{ud}}$  to other nuclear  $\beta$ -decay measurements in Fig. 6. Our  $^{37}\text{K}$  result has the same accuracy as  $^{19}\text{Ne}$  [42] and improves a CVC test at  $I > 1/2$  [51]. Combining the four values from the  $T=1/2$  mirror transitions leads to a new average  $\langle V_{\text{ud}} \rangle_{\text{mirror}} = 0.9727(14)$ , only  $6.7\times$  less precise than the  $0^+ \rightarrow 0^+$  result [16] and slightly better than the neutron.

We have used a highly polarized, laser-cooled source of  $^{37}\text{K}$  to measure the  $\beta$  asymmetry in its decay to be  $A_\beta = -0.5707 \pm 0.0019$ , placing limits on the mass of a hypothetical  $W_R$  coupling to right-handed  $\nu$ 's as well as improving the value of  $V_{\text{ud}}$  from mirror transitions. The high precision of our nuclear polarization measurement on the atom cloud is enabling a further program of improved  $A_\beta$ ,  $B_\nu$ , and recoil asymmetry measurements.

We acknowledge TRIUMF/ISAC staff, in particular for TiC target preparation, and the remaining authors of Ref. [9] for previous polarization development. Supported by the Natural Sciences and Engineering Research Council of Canada, the Israel Science Founda-

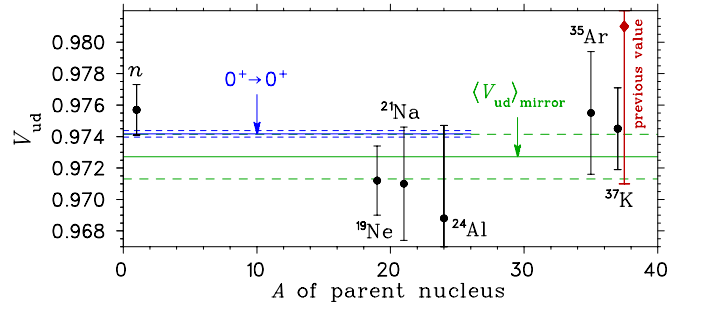


FIG. 6. Measurements of  $V_{\text{ud}}$  comparing the values from the neutron [39],  $^{24}\text{Al}$  [51], and the  $T = 1/2$  mirror nuclei:  $^{19}\text{Ne}$  [42],  $^{21}\text{Na}$  [52],  $^{35}\text{Ar}$  [43], the previous value for  $^{37}\text{K}$  [12], and the present work. The averages (uncertainties) in  $V_{\text{ud}}$  determined from  $0^+ \rightarrow 0^+$  [16] and mirror transitions are shown as the solid (dashed) lines.

tion, and the U.S. Department of Energy, Office of Science, Office of Nuclear Physics under Award No. DE-FG03-93ER40773 and No. DE-FG02-11ER41747. TRIUMF receives federal funding via a contribution agreement through the National Research Council of Canada.

\* dmelconian@tamu.edu

- [1] Barry R Holstein, “Precision frontier in semileptonic weak interactions: introduction and overview,” *J. Phys. G* **41**, 110301 (2014).
- [2] E. Thomas, R. Prieels, M. Allet, K. Bodek, J. Camps, J. Deutsch, F. Gimeno-Nogues, J. Govaerts, J. Lang, O. Naviliat-Cuncic, I. Pepe, P. Quin, N. Severijns, and J. Sromicki, “Positron polarization in the decay of polarized  $^{12}\text{N}$ : a precision test of the Standard Model,” *Nucl. Phys. A* **694**, 559 (2001).
- [3] J. A. Behr and A. Gorelov, “ $\beta$ -decay angular correlations with neutral atom traps,” *J. Phys. G* **41**, 114005 (2014).
- [4] M. G. Sternberg, R. Segel, N. D. Scielzo, G. Savard, J. A. Clark, P. F. Bertone, F. Buchinger, M. Burkey, S. Caldwell, A. Chaudhuri, J. E. Crawford, C. M. Deibel, J. Greene, S. Gulick, D. Lascar, A. F. Levand, G. Li, A. Pérez Galván, K. S. Sharma, J. Van Schelt, R. M. Yee, and B. J. Zabransky, “Limit on tensor currents from  $^8\text{Li}$   $\beta$  decay,” *Phys. Rev. Lett.* **115**, 182501 (2015).
- [5] M. Mehlman, P. D. Shidling, R. Burch, E. Bennett, B. Fenker, and D. Melconian, “Status of the TAMU-TRAP facility and initial characterization of the RFQ cooler/buncher,” *Hyperfine Interact.* **235**, 77 (2015).
- [6] G. Ban, D. Durand, X. Fléhard, E. Liénard, and O. Naviliat-Cuncic, “Precision measurements in nuclear  $\beta$ -decay with LPCTrap,” *Ann. Phys.* **525**, 576 (2013).
- [7] D. Mund, B. Märkisch, M. Deissenroth, J. Krempel, M. Schumann, H. Abele, A. Petoukhov, and T. Soldner, “Determination of the weak axial vector coupling  $\lambda = g_A/g_V$  from a measurement of the  $\beta$ -asymmetry parameter  $A$  in neutron beta decay,” *Phys. Rev. Lett.* **110**, 172502 (2013).
- [8] A. R. Young, S. Clayton, B. W. Filippone, P. Geltenbort, T. M. Ito, C.-Y. Liu, M. Makela, C. L. Morris, B. Plas-

- ter, A. Saunders, S. J. Seestrom, and R. B. Vogelaar, “Beta decay measurements with ultracold neutrons: a review of recent measurements and the research program at Los Alamos National Laboratory,” *J. Phys. G* **41**, 114007 (2014).
- [9] B. Fenker, J.A. Behr, D. Melconian, R.M.A. Anderson, M. Anholm, D. Ashery, R.S. Behling, I. Cohen, I. Craiciu, J.M. Donohue, C. Farfan, D. Friesen, A. Gorelov, J. McNeil, M. Mehlman, H. Norton, K. Olchanski, S. Smale, O. Thériault, A.N. Vantghem, and C.L. Warner, “Precision measurement of the nuclear polarization in laser-cooled, optically pumped  $^{37}\text{K}$ ,” *New J. Phys.* **18**, 073028 (2016).
- [10] J. D. Jackson, S. B. Treiman, and H. W. Wyld, “Possible tests of time reversal invariance in beta decay,” *Phys. Rev.* **106**, 517 (1957); J.D. Jackson, S.B. Treiman, and H.W. Wyld, “Coulomb corrections in allowed beta transitions,” *Nucl. Phys.* **4**, 206 (1957).
- [11] B. Fenker et al. (unpublished).
- [12] P. D. Shidling, D. Melconian, S. Behling, B. Fenker, J. C. Hardy, V. E. Jacob, E. McCleskey, M. McCleskey, M. Mehlman, H. I. Park, and B. T. Roeder, “Precision half-life measurement of the  $\beta^+$  decay of  $^{37}\text{K}$ ,” *Phys. Rev. C* **90**, 032501(R) (2014).
- [13] Meng Wang, G. Audi, F.G. Kondev, W.J. Huang, S. Naimi, and Xing Xu, “The AME2016 atomic mass evaluation (II). tables, graphs and references,” *Chin. Phys. C* **41**, 030003 (2017).
- [14] N. Severijns, M. Tandecki, T. Phalet, and I. S. Towner, “ $\mathcal{F}t$  values of the  $T = 1/2$  mirror  $\beta$  transitions,” *Phys. Rev. C* **78**, 055501 (2008).
- [15] E. Hagberg, I. S. Towner, T. K. Alexander, G. C. Ball, J. S. Forster, J. C. Hardy, J. G. Hykawy, V. T. Koslowsky, J. R. Leslie, H.-B. Mak, I. Neeson, and G. Savard, “Measurement of the  $l$ -forbidden Gamow-Teller branch of  $^{37}\text{K}$ ,” *Phys. Rev. C* **56**, 135 (1997).
- [16] J. C. Hardy and I. S. Towner, “Superallowed  $0^+ \rightarrow 0^+$  nuclear  $\beta$  decays: 2014 critical survey, with precise results for  $V_{ud}$  and CKM unitarity,” *Phys. Rev. C* **91**, 025501 (2015).
- [17] P. Herczeg, “Beta decay beyond the standard model,” *Prog. Part. Nucl. Phys.* **46**, 413 (2001).
- [18] Barry R. Holstein, “Recoil effects in allowed beta decay: The elementary particle approach,” *Rev. Mod. Phys.* **46**, 789 (1974); “Erratum: Recoil effects in allowed beta decay: The elementary particle approach,” *Rev. Mod. Phys.* **48**, 673 (1976).
- [19] I. Towner (private communication).
- [20] J. A. Behr, A. Gorelov, K. P. Jackson, M. R. Pearson, M. Anholm, T. Kong, R. S. Behling, B. Fenker, D. Melconian, D. Ashery, and G. Gwinner, “TRINAT: measuring  $\beta$ -decay correlations with laser-trapped atoms,” *Hyperfine Interact.* **225**, 115 (2014).
- [21] J. A. Behr and G. Gwinner, “Standard model tests with trapped radioactive atoms,” *J. Phys. G* **36**, 033101 (2009).
- [22] T. B. Swanson, D. Asgeirsson, J. A. Behr, A. Gorelov, and D. Melconian, “Efficient transfer in a double magneto-optical trap system,” *J. Opt. Soc. Am. B* **15**, 2641 (1998).
- [23] M. Landini, S. Roy, L. Carcagní, D. Trypogeorgos, M. Fattori, M. Inguscio, and G. Modugno, “Sub-Doppler laser cooling of potassium atoms,” *Phys. Rev. A* **84**, 043432 (2011).
- [24] Matthew Harvey and Andrew James Murray, “Cold atom trap with zero residual magnetic field: The ac magneto-optical trap,” *Phys. Rev. Lett.* **101**, 173201 (2008).
- [25] See the following Supplemental Material for details, which includes Refs. [26, 27].
- [26] J. A. Lonergan, C. P. Jupiter, and G. Merkel, “Electron energy straggling measurements for thick targets of beryllium, aluminum, and gold at 4.0 and 8.0 MeV,” *J. Appl. Phys.* **41**, 678 (1970).
- [27] D. H. Rester and J. H. Derrickson, “Electron transmission measurements for Al, Sn, and Au targets at electron bombarding energies of 1.0 and 2.5 MeV,” *J. Appl. Phys.* **42**, 714 (1971).
- [28] A. Gorelov, J.A. Behr, D. Melconian, M. Trinczek, P. Dubé, O. Häusser, U. Giesen, K.P. Jackson, T. Swanson, J.M. D’Auria, M. Domsbky, G. Ball, L. Buchmann, B. Jennings, J. Dilling, J. Schmid, D. Ashery, J. Deutsch, W.P. Alford, D. Asgeirsson, W. Wong, and B. Lee, “Beta-neutrino correlation experiments on laser trapped  $^{38m}\text{K}$ ,  $^{37}\text{K}$ ,” *Hyperfine Interact.* **127**, 373 (2000).
- [29] A. Gorelov, D. Melconian, W. P. Alford, D. Ashery, G. Ball, J. A. Behr, P. G. Bricault, J. M. D’Auria, J. Deutsch, J. Dilling, M. Domsbky, P. Dubé, J. Fingler, U. Giesen, F. Glück, S. Gu, O. Häusser, K. P. Jackson, B. K. Jennings, M. R. Pearson, T. J. Stocki, T. B. Swanson, and M. Trinczek, “Scalar interaction limits from the  $\beta$ - $\nu$  correlation of trapped radioactive atoms,” *Phys. Rev. Lett.* **94**, 142501 (2005).
- [30] T. J. Gay and F. B. Dunning, “Mott electron polarimetry,” *Rev. Sci. Instrum.* **63**, 1635 (1992).
- [31] B. Plaster, R. Rios, H. O. Back, T. J. Bowles, L. J. Broussard, R. Carr, S. Clayton, S. Currie, B. W. Filippone, A. García, P. Geltenbort, K. P. Hickerson, J. Hoagland, G. E. Hogan, B. Hona, A. T. Holley, T. M. Ito, C.-Y. Liu, J. Liu, M. Makela, R. R. Mammei, J. W. Martin, D. Melconian, M. P. Mendenhall, C. L. Morris, R. Mortensen, R. W. Pattie, A. Pérez Galván, M. L. Pitt, J. C. Ramsey, R. Russell, A. Saunders, R. Schmid, S. J. Seestrom, S. Sjøe, W. E. Sondheim, E. Tatar, B. Tipton, R. B. Vogelaar, B. VornDick, C. Wrede, Y. P. Xu, H. Yan, A. R. Young, and J. Yuan (UCNA Collaboration), “Measurement of the neutron  $\beta$ -asymmetry parameter  $A_0$  with ultracold neutrons,” *Phys. Rev. C* **86**, 055501 (2012).
- [32] S. Agostinelli et al. (GEANT4 Collaboration), “GEANT4 – a simulation toolkit,” *Nucl. Instrum. Methods Phys. Res., Sect. A* **506**, 250 (2003).
- [33] B. Fenker, Ph.D. Thesis, Texas A & M University (2016).
- [34] G. Soti, F. Wauters, M. Breitenfeldt, P. Finlay, I.S. Kraev, A. Knecht, T. Porobi, D. Zkouck, and N. Severijns, “Performance of GEANT4 in simulating semiconductor particle detector response in the energy range below 1 MeV,” *Nucl. Instrum. Methods Phys. Res., Sect. A* **728**, 11 (2013).
- [35] H. W. Lewis, “Multiple scattering in an infinite medium,” *Phys. Rev.* **78**, 526 (1950).
- [36] S. Goudsmit and J. L. Saunderson, “Multiple scattering of electrons,” *Phys. Rev.* **57**, 24 (1940).
- [37] I. Ben-Itzhak, O. Heber, I. Gertner, and B. Rosner, “Production and mean-lifetime measurement of metastable  $\text{Ar}^-$  ions,” *Phys. Rev. A* **38**, 4870 (1988).
- [38] D. Melconian, J.A. Behr, D. Ashery, O. Aviv, P.G. Bricault, M. Domsbky, S. Fostner, A. Gorelov, S. Gu, V. Hanemaayer, K.P. Jackson, M.R. Pearson, and I. Vollrath, “Measurement of the neutrino asymmetry in the  $\beta$  decay of laser-cooled, polarized  $^{37}\text{K}$ ,” *Phys. Lett. B* **649**, 370 (2007).

- [39] C. Patrignani et al. (Particle Data Group), “Review of particle physics,” *Chin. Phys. C* **40**, 100001 (2016).
- [40] N. Severijns and O. Naviliat-Cuncic, “Symmetry tests in nuclear beta decay,” *Annu. Rev. Nucl. Part. Sci.* **61**, 23 (2011).
- [41] F. P. Calaprice, S. J. Freedman, W. C. Mead, and H. C. Vantine, “Experimental study of weak magnetism and second-class interaction effects in the  $\beta$  decay of polarized  $^{19}\text{Ne}$ ,” *Phys. Rev. Lett.* **35**, 1566 (1975).
- [42] L. J. Broussard, H. O. Back, M. S. Boswell, A. S. Crowell, P. Dendooven, G. S. Giri, C. R. Howell, M. F. Kidd, K. Jungmann, W. L. Kruithof, A. Mol, C. J. G. Onderwater, R. W. Pattie, P. D. Shidling, M. Sohani, D. J. van der Hoek, A. Rogachevskiy, E. Traykov, O. O. Versolato, L. Willmann, H. W. Wilschut, and A. R. Young, “Measurement of the half-life of the  $T = \frac{1}{2}$  mirror decay of  $^{19}\text{Ne}$  and its implication on physics beyond the standard model,” *Phys. Rev. Lett.* **112**, 212301 (2014).
- [43] O. Naviliat-Cuncic and N. Severijns, “Test of the conserved vector current hypothesis in  $T = 1/2$  mirror transitions and new determination of  $|V_{ud}|$ ,” *Phys. Rev. Lett.* **102**, 142302 (2009).
- [44] A. S. Carnoy, J. Deutsch, T. A. Girard, and R. Prieels, “Limits on nonstandard weak currents from the positron decays of  $^{14}\text{O}$  and  $^{10}\text{C}$ ,” *Phys. Rev. Lett.* **65**, 3249 (1990).
- [45] F. Wauters, V. DeLeebeeck, I. Kraev, M. Tandecki, E. Traykov, S. VanGorp, N. Severijns, and D. Zákoucký, “ $\beta$  asymmetry parameter in the decay of  $^{114}\text{In}$ ,” *Phys. Rev. C* **80**, 062501 (2009).
- [46] F. Wauters, I. Kraev, D. Zákoucký, M. Beck, M. Breitenfeldt, V. De Leebeeck, V. V. Golovko, V. Yu. Kozlov, T. Phalet, S. Roccia, G. Soti, M. Tandecki, I. S. Towner, E. Traykov, S. Van Gorp, and N. Severijns, “Precision measurements of the  $^{60}\text{Co}$   $\beta$ -asymmetry parameter in search for tensor currents in weak interactions,” *Phys. Rev. C* **82**, 055502 (2010).
- [47] G. Soti, F. Wauters, M. Breitenfeldt, P. Finlay, P. Herzog, A. Knecht, U. Köster, I. S. Kraev, T. Porobic, P. N. Prashanth, I. S. Towner, C. Tramm, D. Zákoucký, and N. Severijns, “Measurement of the  $\beta$ -asymmetry parameter of  $^{67}\text{Cu}$  in search for tensor-type currents in the weak interaction,” *Phys. Rev. C* **90**, 035502 (2014).
- [48] J. F. Bueno et al. (TWIST Collaboration), “Precise measurement of parity violation in polarized muon decay,” *Phys. Rev. D* **84**, 032005 (2011).
- [49] Takehiko Asaka and Mikhail Shaposhnikov, “The  $\nu\text{MSM}$ , dark matter and baryon asymmetry of the universe,” *Phys. Lett. B* **620**, 17 (2005).
- [50] M. Konieczka, P. Baczyk, and W. Satuła, “ $\beta$ -decay study within multireference density functional theory and beyond,” *Phys. Rev. C* **93**, 042501 (2016).
- [51] E. G. Adelberger, P. B. Fernandez, C. A. Gossett, J. L. Osborne, and V. J. Zeps, “Does the Cabibbo angle vanish in Fermi matrix elements of high- $J$  states?” *Phys. Rev. Lett.* **55**, 2129 (1985).
- [52] J. Grinyer, G. F. Grinyer, M. Babo, H. Bouzomita, P. Chauveau, P. Delahaye, M. Dubois, R. Frigot, P. Jardin, C. Leboucher, L. Maunoury, C. Seiffert, J. C. Thomas, and E. Traykov, “High-precision half-life measurement for the isospin  $T = 1/2$  mirror  $\beta^+$  decay of  $^{21}\text{Na}$ ,” *Phys. Rev. C* **91**, 032501 (2015).

**Supplemental Material for *Precision Measurement of the  $\beta$  Asymmetry in Spin-Polarized  $^{37}\text{K}$  Decay***

B. Fenker, A. Gorelov, D. Melconian, J.A. Behr, M. Anholm, D. Ashery, R.S. Behling, I. Cohen, I. Craiciu, G. Gwinner, J. McNeil, M. Mehlman, K. Olchanski, P.D. Shidling, S. Smale, and C.L. Warner

**ATOMIC PHYSICS**

Given the precision measurement of our Letter, we include here some additional details about the atomic physics methods for the interested reader. Certain atomic effects produce negligible uncertainties on the determination of the nuclear polarization  $P$  needed to deduce the value of  $A_\beta$  for  $^{37}\text{K}$ , and we explore these through more detailed measurements made possible by larger quantities of stable  $^{41}\text{K}$  atoms. We take the opportunity to provide some qualitative guides to our detailed publication on our polarization methods in Ref. [1].

There are several features of our optical pumping and probing method that we want to emphasize. We probe the small unpolarized fraction, so not much precision is required. Our probe is parasitic — unlike most more direct methods, it does not alter the polarization during probing. We also measure  $P$  throughout the duty cycle of polarization, so we can choose the best times of the duty cycle to determine  $A_\beta$ .

**Optical pumping tests on stable  $^{41}\text{K}$**

*Qualitative description*

For optical pumping of small densities of atoms, there are two depolarization mechanisms. We measure optically the degree of imperfectly circularly polarized light (see Section 2.3 of Ref. [1]). We then fit the excited state population mentioned in our Letter for a parameter  $B_x$ , an average magnetic field perpendicular to the optical pumping  $\hat{z}$  axis. The result, after a full detailed characterization of optical pumping using the well-established optical Bloch equations (OBE, described in Ref. [1]), determines the population of unpolarized atomic states. Most important is the population of two almost-pumped ground states ( $F=2$   $M_F=1$  and  $F=1$   $M_F=1$ ) with nuclear polarization  $1/2$  and  $5/6$ : determining their population supplies the precision needed for this Letter. Larmor precession governed by  $B_x$  does not change  $F$ , while the measured imperfect circular polarized light can change  $F$  by optical pumping, so once we quantify the two depolarization mechanisms the OBE's give us the populations we need.

The tail/peak ratio of the excited state population determines  $1 - P$ . Given that  $1 - P$  is less than 0.01, and

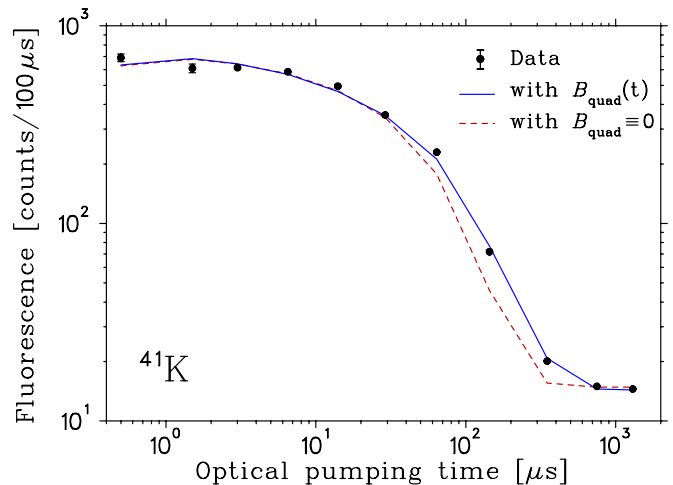


FIG. S1. Fluorescence of  $^{41}\text{K}$  in  $4S_{1/2}$  to  $4P_{1/2}$  transition during optical pumping. Note the log-log scale showing the peak fluorescence, the region dominated by falling  $B_x[t]$ , and the tail due to imperfect polarization.

that the nuclear polarization is  $\geq 0.5$  for the two almost-pumped unpolarized states, we only need on order 10% accuracy on the tail/peak ratio to achieve the result of Ref. [1],  $1 - P = 0.0087 \pm 0.0009$ . If there were no excited state fluorescence in  $^{41}\text{K}$  at long times in Fig. S1 (or photoions in  $^{37}\text{K}$  in Ref. [1]), the polarization would be 100% with no uncertainty.

Thus effectively, a single parameter,  $B_x$ , is fit to the  $^{37}\text{K}$  excited state population data. All other parameters are fixed by independent measurements on  $^{37}\text{K}$ , and high-statistics independent data on  $^{41}\text{K}$  in the same geometry. The  $^{41}\text{K}$  data we describe in this Supplemental Material is helpful in lending confidence to our model, but in the end not essential to the  $^{37}\text{K}$  polarization result.

*Time dependence of  $B_x$*

We mention in Section 2.3 of Ref. [1] that we measure the time-dependence of  $B_x$  with Hall probes as the MOT quadrupole  $B$  field falls. This provides reasonable accuracy, albeit with vacuum system open without detectors installed, and suggests the depolarization from this component is unimportant in the part of the duty cycle used for  $A_\beta$  data.

To test this with all detectors in place, we optically pump stable  $^{41}\text{K}$  atoms.  $^{41}\text{K}$  has almost the same hyperfine structure as  $^{37}\text{K}$ , so after adjusting laser frequencies experimentally the OBE predict almost the same results. We show in Fig. S1 the dependence of the fluorescence of the  $4P_{1/2}$  state as a function of time, along with optical pumping calculations including the time dependence of  $B_x$ . The region from 60 to 200  $\mu\text{s}$  after the optical pumping starts is better modelled if we include this time-changing  $B_x$ , with the fall time fixed to the Hall



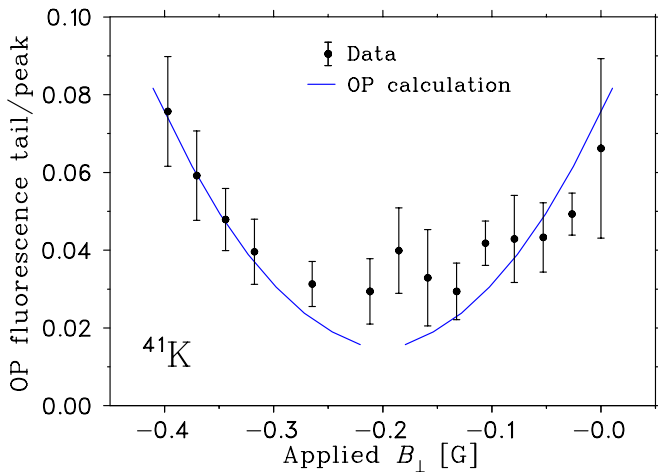


FIG. S2. Optical pumping tail/peak ratio for  $^{41}\text{K}$ , optimized by changing one set of uniform-field Helmholtz coils.

probe measurement of  $\tau = 130 \mu\text{s}$ . In Fig. S1 the MOT quadrupole field was turned off at  $-250 \mu\text{s}$ . We waited longer for the MOT field to decay away before we started optical pumping  $^{37}\text{K}$  (see Fig. 10 of Ref. [1]), and then simply waited for this field to decay away to take the  $A_\beta$  data. The tail/peak ratio, and hence the deduced polarization of  $^{37}\text{K}$  at OP times used for  $\beta$  decay, do not depend on whether or not the decaying MOT quadrupole field is included in the theory. Nor is the goodness of fit with and without this effect changed in the  $^{37}\text{K}$  photoion data (Fig. 8 and Fig. 10 of Ref. [1]).

With data of this sort, we can tune parameters to optimize the polarization. Figure S2 shows optimization of one perpendicular uniform magnetic  $B$  field by trimming the current through a Helmholtz coil along one perpendicular axis, after similar optimization of the other axis. This effectively aligns the total  $\mathbf{B}$  field with the OP laser light axis. The OP laser light axis is in turn aligned mechanically with the  $\beta$  detector axis, to optical alignment accuracy of 1 mm in 1 m, or 0.001 rad, producing negligible misalignment accuracy on  $\cos\theta_{\beta\hat{f}}$  of less than  $10^{-6}$ .

We also learn that the polarization difference from unity depends quadratically on applied  $B_\perp$ , in agreement with our OP calculation. The result in Fig. S2 is consistent with a small average horizontal field that is not zeroed out with our uniform applied field. In our  $^{37}\text{K}$  data we are also able to fit for this effective  $B_x$ , and find it is consistent with the values found for  $^{41}\text{K}$ , as would be expected since the atom clouds are located at almost the same position in the apparatus.

*Spatial gradients of the  $B$  field* Given the dying remnants of the time-changing MOT quadrupole field, it is natural to consider whether spatial gradients of the magnetic field can make gradients of the polarization across the atom cloud. In particular, a finite  $dP/dz$  could in principle perturb  $A_\beta$  significantly. However, the possible residual  $dB/dz$  of  $< 0.01 \text{ G/cm}$  detunes the optical

pumping laser by negligible Zeeman shifts, so negligible  $dP/dz$  is produced. For measurement of future  $\beta$ -decay observables, polarization gradients along the other axes are being studied (by fast CMOS camera) and minimized (by the standard trick of unbalancing Helmholtz coils).

### Metastable $\text{Ar}^-$ atoms

If nothing else happens,  $\beta^+$  decay of a potassium atom populates a negative Ar ion. The ground state of this ion is, of course, unstable, and dissociates in negligible time. There is a known metastable state of the  $\text{Ar}^-$  ion with lifetime  $\tau = 260 \text{ ns}$  [2]. We mention here that this state makes negligible contribution to  $A_\beta$  systematic uncertainties.

The angular distribution of the  $\beta^+$  is quite different in singles versus in coincidence with the recoil (i.e. the  $\nu$ ). So it is important in measuring  $A_\beta$  that the shakeoff electrons be detected with no bias from the recoil direction. A metastable  $\text{Ar}^-$  could in principle move in  $z$  first before releasing the electron, thus biasing the critical coincidence.

We can fit for a tail with the known lifetime in the  $\beta$ -shakeoff electron TOF spectra like Fig. 4 of our Letter (but to longer times than shown). The population of the  $\text{Ar}^{-1}$  is less than 4%, which could produce a less than 0.08% correction to  $A_\beta$  using a 40-mm diameter shakeoff electron detector. However, such a tail is excluded by the time width of the  $\beta$ -shakeoff coincidence in Fig. 4 used for  $A_\beta$ , so the possible distortion to  $A_\beta$  vanishes.

### $\beta$ (BACK)SCATTERING

A primary concern of any  $\beta$  asymmetry measurement is the effect of  $\beta$  scattering before entering the detector. These events will have an apparent initial direction that is incorrect and will therefore bias the results – especially in the case of large-angle backscatters. A separate publication is in preparation where we will describe in greater detail our estimates of these effects [3], but in order for the reader of our Letter to understand how we arrived at the correction and uncertainty for  $\beta$  scattering in Table I of the Letter, we provide the plots comparing our data to our GEANT4 simulation which led to these results.

One comparison of the data to GEANT4 could be made by looking at events where the  $\beta$  backscatters off of one double-sided Si-strip detector (DSSSD) into the both the scintillator and DSSSD of the opposite  $\beta$  telescope. However, given the small ( $\sim 0.25\%$ ) solid angle for a  $\beta$  to go from one telescope to the other, these events are extremely rare,  $\lesssim 10^{-4}$  of non-scattering events. The effect of  $\beta$  backscattering on the  $A_\beta$  measurement in our geometry is highly suppressed: the 20 candidate events in our data set are too few to serve as a meaningful benchmark

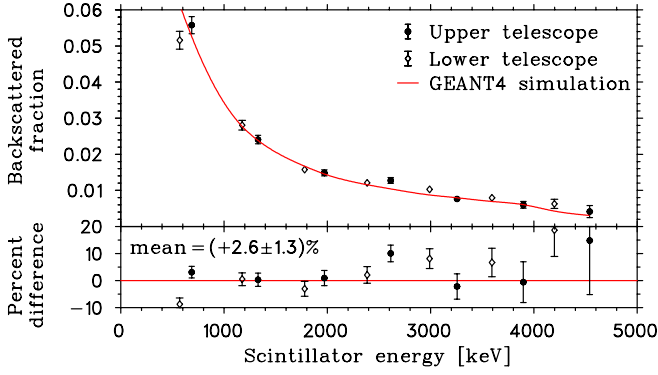


FIG. S3. Comparison of GEANT4 with the observed fraction of events backscattering out of the scintillator through a 2nd pixel in the DSSSD  $\Delta E$  detector. The bottom plot shows the percent difference between GEANT4 and observations.

for GEANT4. Although negligible, these events were vetoed in the analysis of  $A_\beta$ .

A much more frequent type of backscatter we are able to measure experimentally are events in one  $\beta$  telescope where the scintillator and two pixels in the corresponding DSSSD are all above threshold [4]. These “scintillator-backscatter” events correspond to a  $\beta$  entering a pixel in the DSSSD of one of the  $\beta$  telescopes, leaving energy in the plastic scintillator, and then backscattering out through a different pixel of the same DSSSD detector. Note that this is a very clean measurement: the triple-coincidence between the shake-off electron MCP, the DSSSD and the scintillator greatly suppresses  $\gamma$  events and other backgrounds, and in particular the shake-off electron coincidence ensures the decay occurred from the trap.

Figure S3 shows the fraction of scintillator-backscatter events normalized to the number of good events as observed by each  $\beta$  telescope. These are compared to the fraction predicted by the GEANT4 simulation, which can be seen to be quite favourable when using the non-standard GEANT4 options listed in the Letter: the average difference is only  $(+2.6 \pm 1.3)\%$  over the range of energies considered in our analysis. This unique measurement of backscattering out of plastic scintillator serves as our benchmark for testing the efficacy of our GEANT4 simulations.

The same GEANT4 simulation is used to predict the effect of  $\beta$  scattering on the  $A_\beta$  measurement. Given the position of an event in the DSSSD and assuming the decay occurred from the trap center, we are able to calculate the angle between the polarization direction and the momentum of the  $\beta$ . If the  $\beta$  scattered before entering the detector, this calculated angle will be wrong, most dramatically for events which backscattered off of a volume opposite the telescope in which it was detected. To estimate the effect, we performed a simulation looking at events which fired the  $\beta$  telescope in the same direction

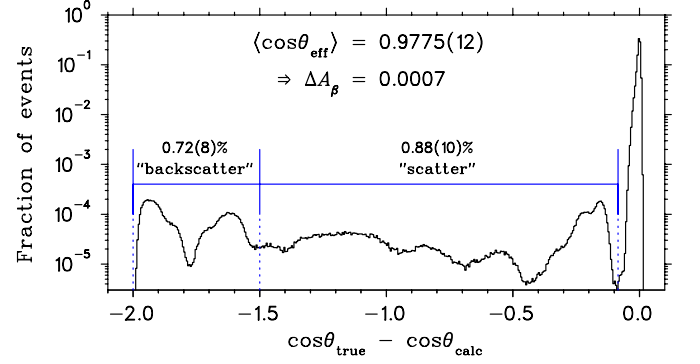


FIG. S4. GEANT4 simulation showing the effect on the  $A_\beta$  measurement due to  $\beta$  scattering. The dominant peak at  $\Delta \cos \theta \approx 0$  are events which entered the  $\beta$  telescope directly from the trap; the events below this peak are ones where the  $\beta$  scattered before entering the detector and which lead to an incorrect angle reconstruction. We have divided these events into two regions: 0.72(8)% of events we labelled “backscatter” events, and 0.88(10)% “scatter” (see text). Instead of the true  $\cos \theta$ ,  $\beta$ -scattering effects lead to an effective  $\cos \theta$  that is attenuated by 2.3%.

as the initial nuclear polarization (so  $\cos \theta_{\text{calc}} \approx 1$ ) and compared this to the actual  $\cos \theta$  of the generated event.

Figure S4 shows the distribution of simulated events as a function of the true  $\cos \theta$  minus that which we calculate based on the position in the DSSSD. The main peak at  $\Delta \cos \theta \approx 0$ , containing 98.40(12)% of the spectrum, are events which entered the  $\beta$  telescope with minimal scattering; most of the width of this peak is due to the finite position resolution of the DSSSD (1 mm strips) and finite size of the cloud of atoms. The events below this main peak correspond to events which scattered off the opposite  $\beta$  telescope, one of the electrostatic hoops and/or one of the other volumes shown in Fig. 1 of the Letter.

All together, GEANT4 predicts that scattered events reduce the observed asymmetry by  $1/\langle \cos \theta_{\text{eff}} \rangle = 1.0230$ . Our analysis, based on these GEANT4 simulations, includes this 2.30% correction for  $\beta$  scattering. To assign a systematic uncertainty, we consider three regions in Fig. S4: “not scattered” events are those where  $\Delta \cos \theta \geq -0.085$ ; “backscattered” events are those where  $\Delta \cos \theta \leq -1.5$ ; and the rest,  $-1.5 < \Delta \cos \theta < -0.085$  are “scattered”. We varied the fraction of events in the “scattered” and “backscattered” regions to estimate a systematic uncertainty on  $\langle \cos \theta_{\text{eff}} \rangle$ . For the “backscattered” region, we use our result from Fig. S3 to assign an uncertainty of 5.1%, the  $2\sigma$  upper-limit of the difference shown. We have no data of our own to constrain the fraction of “scattered” events, so for these we assign a 10% uncertainty, consistent with the accuracy of a GEANT4 simulation we ran compared to literature data on few MeV electron transmission through thin materials into angles of 10 – 75 degs [5, 6]. The result is a  $\pm 0.0012$

uncertainty on  $\langle \cos \theta_{\text{eff}} \rangle$  and an absolute systematic uncertainty of  $\pm 0.0007$  on  $A_\beta$ , which is 5.6% of the total correction. This is the systematic uncertainty assigned directly to  $\beta$  scattering in Table I of the Letter. Note that there are five other entries in this table of uncertainties (labelled with a superscript “a”) which also contribute to  $\beta$  scattering, albeit to a lesser extent and less directly.

---

\* [dmelconian@tamu.edu](mailto:dmelconian@tamu.edu)

- [1] B. Fenker, J.A. Behr, D. Melconian, R.M.A. Anderson, M. Anholm, D. Ashery, R.S. Behling, I. Cohen, I. Craiciu, J.M. Donohue, C. Farfan, D. Friesen, A. Gorelov, J. McNeil, M. Mehlman, H. Norton, K. Olchanski, S. Smale, O. Thériault, A.N. Vantghem, and C.L. Warner, “Precision measurement of the nuclear polarization in laser-cooled, optically pumped  $^{37}\text{K}$ ,” [New J. Phys. \*\*18\*\*, 073028 \(2016\)](#).
- [2] I. Ben-Itzhak, O. Heber, I. Gertner, and B. Rosner, “Production and mean-lifetime measurement of metastable  $\text{Ar}^-$  ions,” [Phys. Rev. A \*\*38\*\*, 4870 \(1988\)](#).
- [3] B. Fenker, A. Gorelov, D. Melconian, J.A. Behr, M. Anholm, D. Ashery, R.S. Behling, I. Cohen, I. Craiciu, G. Gwinner, J. McNeil, M. Mehlman, K. Olchanski, P.D. Shidling, S. Smale, and C.L. Warner, (unpublished).
- [4] B. Fenker, Ph.D. Thesis, Texas A & M University (2016).
- [5] J. A. Lonergan, C. P. Jupiter, and G. Merkel, [J. App. Phys. \*\*41\*\*, 678 \(1970\)](#).
- [6] D. H. Rester and J. H. Derrickson, [J. App. Phys. \*\*42\*\*, 714 \(1971\)](#).